American Journal of Biomedical Engineering 2026, 14(1): 9-15
DOI: 10.5923/j.ajbe.20261401.02

Synthesis and Characterization of Hydroxyapatite from Dolomite-based Source for Bone Regeneration

Chinenye Appolonia Ibekwe[1,*], Grace Modupe Oyatogun[1], Temitope Ayodeji Esan[2], Elizabeth Obhioneh Oziegbe[3]

[1]Department of Materials Science and Engineering, Faculty of Technology Obafemi Awolowo University, Ile-Ife, Osun State, Nigeria
[2]Department of Restorative Dentistry, Faculty of Dentistry, Obafemi Awolowo University, Ile-Ife, Osun State, Nigeria
[3]Department of Child Dental Health, Faculty of Dentistry, Obafemi Awolowo University, Ile-Ife, Osun State, Nigeria

Abstract This study synthesized and characterized hydroxyapatite (HAp) from Nigerian-based dolomite with the view investigating its suitability for a scaffold development for bone regeneration. The dolomite was pulverized and calcined at 900 ℃ to obtain calcium oxide, which was used to synthesize HAp by the wet chemical precipitation method. Furthermore, the chemical characterization of pulverized dolomite and HAp was done using X-ray Fluorescence (XRF) and X-ray Diffraction (XRD) Spectroscopy techniques. In addition, Fourier Transform Infrared (FT-IR) was used to examine the functional group of HAp while the morphological characterization was achieved by Scanning Electron Microscopy (SEM) technique. Moreover, the XRD and XRF results confirmed the presence of calcite and magnesium in dolomite while they also confirmed HAp in synthesized dolomite-based HAp, which was supported by the FT-IR spectrum that showed the presence of phosphate compound with peaks at 1122.6, 1041.6, 991.4, 605.7 and 559.5 cm^{-1} while the presence of hydroxyl was revealed with peak 3468.1 cm^{-1}. Furthermore, the XRF results showed that the Ca/P molar ratio was more than 1.67, which was close to that of natural bone. The SEM micrograph displayed agglomerated rod structures that resulted in a rough surface, which will facilitate the adhesion and proliferation of bone cells. The study, therefore, affirmed that the dolomite-based hydroxyapatite has similar characteristics to bone hydroxyapatite and may be suitable for the scaffold fabrication for bone regeneration.

Keywords Bone regeneration, Dolomite, Hydroxyapatite and scaffold

1. Introduction

Orthopedic and dental treatments and reconstruction, including bone repair and bone regeneration, often require the use of implant materials, such as metals, ceramics, polymers and composites, that are biocompatible, biodegradable and osteoconductive [1]. Of these, the most frequently researched are ceramics, with hydroxyapatite (HAp) gaining wide attention due to its close similarity with the inorganic component of bone that results in its excellent biocompatibility [1,2,3]. HAp possesses theoretical formula of $Ca_{10}(PO_4)_6(OH)_2$, hexagonal crystal lattice [2-4] and density of between 3.14-3.16 g/cm^3 [4]. These features are responsible for its excellent biological properties, which enhance its biomedical application [2,4].

HAp is either extracted from natural sources, such as bone, shells and fish scale [1,5] or synthesized in the laboratory using materials with high calcium components, such as solid minerals [5,6]. Calcite-bearing minerals, such as limestone, marble and dolomite, are precipitated calcium carbonate of both plant and animal remains and have been utilized in the synthesis of HAp [6-8]. Dolomite is an inorganic and rock-forming crystal comprising of calcium magnesium carbonate ($CaMg(CO_3)_2$) [9]. It has been used to synthesize magnesium-substituted hydroxyapatite, which has been established to have anti-microbial properties due to the presence of magnesium [8]. Although it is widely available in Nigeria [10], it is widely utilized in the industrial sector, such as construction, fertilizer and cements production [11,12] but limited documentation exists on its biomedical application.

Dolomite has been reported to be abundant in Ikpeshi, Edo State [12], which lies within latitudes 7 °06′00″N to 7 °20′00″N and longitudes 6 °08′30″E to 6 °20′64″E southern Nigeria [12]. Extensive studies have been carried out on the mineralogical composition, physical and chemical properties Nigerian-based dolomite [11,12]. Johnson *et al.* [12] studied the mineralogical characterization of the Ikpeshi deposit and observed that the deposit consists of 84.0 wt % dolomite with traces of other minerals, such as calcite (8. 0wt%) and quartz (8.0 wt%). Similarly, Omoseebi and Tanko [10] carried out geochemical analyses on Ikpeshi deposit and reported that

* Corresponding author:
chibek2020@yahoo.com (Chinenye Appolonia Ibekwe)
Received: Jan. 31, 2026; Accepted: Feb. 19, 2026; Published: Feb. 24, 2026
Published online at http://journal.sapub.org/ajbe

the average concentration of the elemental oxides, such as silicon oxide (SiO_2), aluminum oxide (Al_2O_3), iron oxide (Fe_2O_3), manganese oxide (MnO), magnesium oxide (MgO) and calcium oxide (CaO) present in the dolomite were 1.790, 0.461, 0.299, 0.045, 20.380 and 46.130 respectively. All these results confirmed the abundance of CaO and MgO in the mineral, which makes it a good candidate as a raw material for HAp synthesis. Unfortunately, there is little or no evidence to show that HAp can be synthesized from Nigerian-based dolomite. Hence, this work attempted to synthesize HAp using this abundant solid mineral.

The conversion of $CaCO_3$ in calcite-bearing minerals to HAp, firstly involves calcination at high temperature of 900 ℃ to obtain its oxide [6,13], followed by other method, such as sol-gel, hydrothermal and wet chemical precipitation methods [1,3,6,13-15]. Hydrothermal technique involves the HAp precipitation in hydrated solution at elevated temperature and pressure to create an extremely crystalline artifact with a homogeneous chemical composition [16]. However, this method is costly due to its high energy consumption and use of specialized equipment, such as autoclaves [13]. Sol-gel method is another method but it utilizes costly reagents and produces low crystallized product [17]. Meanwhile, wet chemical precipitation method is frequently employed for the synthesis of medical-grade HAp due to ease of technology, low reaction temperature, reduced cost, and most importantly, high purity of the final product [17]. Consequently, this method was adapted for the synthesis of dolomite-based HAp in this study.

The purity, crystallinity and morphology of HAp affect its biocompatibility and mechanical properties [18]. Pure HAp has calcium phosphorous ratio (Ca/P) of 1.67 and is thermodynamically stable in its crystalline state [19,20]. On the other hand, HAp products Ca/P ratio may be higher or less than 1.67, which signifies presence of CaO or TCP respectively [19]. This affects the mechanical properties [20] and the biocompatibility of the scaffold [18]. TCP has low mechanical properties and non-stable in physiological fluid while CaO has high mechanical properties. In addition, it is worthy knowing that natural HAp is non-stoichiometric, which is as a result of either deficiency in calcium or phosphorus ion that is attributed to substitution of trace element [20]. Furthermore, crystallinity of HAp is an important parameter because it affects degradation of a scaffold thereby determining the mechanical properties of a scaffold [21]. Studies have shown that crystalline HAp is bio-inert and less degradable; however, very low heat treated HAp may result in amorphous effect and their degradation in the form of macro-particle release is likely to cause cellular damages around an implanted scaffold [22]. This implies that right crystallinity of HAp is needed for bone regeneration. Moreover, since the osteoblast cells of the bone are sensitive to the physical properties of their surroundings, including surface composition, surface energy, roughness and topography, it is essential to have the right morphology of HAp [23]. This demands imitation of the bone hydroxyapatite crystals, which are plate-or needle-shaped with varying size and shapes. This contributes to their structural stability, hardness and functions [23]. Therefore, it is necessary to synthesis HAp with composition, crystallinity and morphology of bone HAp, which may lead to the competing mechanical and the biological requirements need to rapidly stimulate healing of bone defects.

In essence to have a pure, right morphology and right crystallinity, factors, such as reaction temperatures, sintering temperatures and pH of the solution, must be optimized [24]. Rodriguez-lugo *et al.* [25] examined the effect of reaction pH on purity and particle size of HAp, and observed that there is no relationship between the reaction pH and particle size. They, however, reported that pure HAp could only be synthesized at the pH of 10. Similarly, Wang *et al.* [26] examined the pH effect on HAp morphology, purity and particle size. The TEM image obtained by their study revealed sphere-like nanoparticles structures at the pH of 10 and 11 while aggregated nanowires and rectangular fragments at lower pH of 9 and 8, which was in consistence with the XRD spectra that revealed HAp peaks at pH of 10 while mixture of HAp and other phases peaks at the pH below or above 10. Rafie and Nordin [27] confirmed this finding by obtaining pure HAp at the pH of 10. Thus, the authors confirmed pH of 10 as the optimal value for the synthesis of pure HAp. Furthermore, effect of reaction temperature on purity, morphology and crystallinity of HAp was investigated by Wang *et al.* [26] and their TEM images revealed change from a mixture of spherical and rod-like to bamboo-leaf-like structure as the temperature changed from 25 ℃ to 80 ℃ while their XRD spectra revealed change from amorphous phase to crystalline phase as the temperature increased from 25 to 80 ℃. This finding implies that the HAp purity, crystallinity and particle size increase with a rise in the reaction temperature, which was corroborated by Jamarun *et al.* [28] and Gyorgy *et al.* [30]. Jamarun *et al.* [28] also reported 90 ℃ as the optimal reaction temperature for HAp synthesis. This was corroborated by Kazemzadeh *et al.* [31], who also reported 90 ℃ as the optimal reaction temperature for synthesis of highly purity crystalline HAp.

Moreover, scholars have found that HAp purity, crystallinity and particle size, are affected by the sintering temperature [26]. In a study on the effect of sintering temperature on the HAp morphology, Rodriguez-lugo [25] reported that SEM images changed from semi-acicular to a grain-like structure as the sintering temperature increased. Rafie and Nordin [27] confirmed this finding by reporting a change from needle-like particle size of 83 nm to the sphere-like structure of particle size of 228 nm as sintering temperature increased. This trend has been reported by several researchers [2,21,26,27], consequently the evidence that increase in particle size and crystallinity with a rise in sintering temperature was confirmed. In addition, Indrani *et al.* [21] established 900 ℃ as optimal sintering temperature for HAp, above which resulted in HAp along with secondary phases, such as tri-calcium phosphate. Alias *et al.* [29] supported this finding by observing a shift in the XRD spectrum peaks for the sample sintered at 1000 ℃, which

signifying the HAp dehydroxylation. Consequently, 900 ℃ was established as the ideal sintering temperature for HAp by these authors. Hence, the established optimal parameters, including pH of 10, reaction temperature of 90 ℃ and sintering temperature of 900 ℃ were utilized for synthesis of dolomite-based hydroxyapatite with intention to obtain pure, medical-grade HAp.

2. Materials and Methods

2.1. Materials

The dolomite utilized as source of calcium precursors for this study was obtained from Ikpeshi in Delta state of Nigeria. The choice of this location was due to massive deposit of this mineral. Ortho-phosphoric acid, nitric acid and ammonium (as a regulator) of analytical grade were utilized in the study while distilled water was the only solvent used throughout the synthesis. The magnetic stirrer, centrifuge, oven and furnace were the equipment used in this work.

2.2. Methods

This study synthesized HAp with dolomite by calcination and wet chemical precipitation method.

2.2.1. Calcination

The solid mineral was pulverized, sieved and subsequently 1000 grams of pulverized minerals were calcined at 900 ℃ for 3 hours to convert to its oxide, see equation (i) for the calcination reaction.

$$CaMg(CO_3)_{2(s)} + Heat \rightarrow CaO_{(s)} + MgO_{(s)} + 2CO_{2(g)} \quad (1)$$

2.2.2. Synthesis of Hydroxyapatite

Sirait *et al*. [6] proceedure was used for synthesis of HAp using wet chemical precipitation method. However, due to low solubility, 0.8 M of nitric acid was used to leach out calcium from the dolomite. This method involves dissolving 11.84 g of calcined dolomite with 0.8 M of nitric acid of 200 mls, followed by stirring with a magnetic stirrer for 30 minutes before separation of the filtrate from mixture. The pH of the filtrate was adjusted to 10 with 1M of ammonium solution and 0.3 M of phosphoric acid was added drop wise at rate of 5 mls per minute. Subsequently, the ammonium solution of 1M was used to precipitate HAp from the solution at 90 ℃ and pH of 10. The precipitate was left to age for 24 hours before it was washed, dried and finally sintered at 900 ℃. See equation *ii-iv* for synthesis reactions.

$$CaO(s) + MgO_{(s)} + 4HNO_{3(aq)} \rightarrow Ca\,(NO_3)_{2(aq)} + Mg(NO_3)_{2\,(aq)} + H_2O_{(l)} \quad (2)$$

$$Ca(NO_3)_{2\,(aq)} + Mg(NO_3)_{2(aq)} + 2NH_4OH_{(l)} \rightarrow Ca(OH)_{2\,(aq)} + Mg(OH)_2 + 2NH_4NO_{3(aq)} \quad (3)$$

$$10 - x\;Ca(OH)_{2\,(aq)} + xMg(OH)_{2(aq)} + 6H_3PO_{4\,(l)} \rightarrow Ca_{10-x}Mg_x(PO_4)_6(OH)_{2\,(s)} + 18H_2O_{(l)} \quad (4)$$

2.3. Material Characterization

2.3.1. X-ray Diffraction (XRD) Characterization

The phase composition of dolomite and HAp was studied by XRD using Cu Kα radiation (λ = 0.154 nm). The samples were tested following ASTM-E915-10, which involved mounting the powder on the microscope slide face using a suitable amorphous binder, such as 10% solution of nitrocellulose cement diluted with acetone while the specimen surface was made as smooth as possible. The sample was scanned with 2Θ ranging from 20 °to 80 °at a scan step of 2 per minute and the XRD pattern was generated at the voltage of 40 KV and current of 30 mA. The particle size, surface area and crystallinity of synthesized HAp were done with XRD data using Equation v, vi and vi respectively [32].

$$t = \frac{(0.9)\lambda}{\beta c\, cos\theta} \quad (5)$$

[Where: t is the particle size, λ is the wavelength used, β (FWHM) is peak width and θ is the Bragg diffraction angle].

$$s = \frac{6\times10^3}{dp} \quad (6)$$

[Where: S is the specific surface area (m^2/g), p is the crystal size and d is the theoretical density of HAp (3.16 g/cm^3)].

The crystalline HAp phase (Xc) fraction was calculated using Equation vi [32].

$$x_c = 1 - \frac{V_{112/300}}{I_{300}} \quad (7)$$

[where I_{300} is the intensity of (300) reflection and $V_{112/300}$ of the hollow between (112) and (300) reflections].

Also, the unit cell parameter (a, b) was calculated using Bragg's law as shown in Equation vii [32] and [34].

$$\frac{4sin^2\theta}{\lambda^2} = \frac{4}{3}\left[\frac{h^2+hk+K^2}{a^2}\right] + \left[\frac{L}{c}\right]^2 \quad (8)$$

2.3.2. X-ray Fluorescence (XRF) Characterization

The pulverized dolomite and synthesized HAp elemental composition were determined using XRF technique based on the ASTM C114-11 standard, which involved grinding the XRF samples into fine grains, followed by mixing it with binder in the ratio of 10 to 1 from which four grams were pressed using an aluminum ring in order to obtain tubular pellets suitable for the EDX3600B X-ray fluorescence spectrometer. Each of the pellets from the different samples was mounted on the sample holder's and was irradiated by an intense X-ray beam from the fixed tube at operating conditions of 25 KVA and 6 MA for 20 minutes. The test outcome was presented on the computer connected to X-ray fluorescence spectrometer, which recorded the elements percentage.

2.3.3. Fourier Transform Infrared (FT-IR) Characterization

The functional groups present in synthesized HAp were examined using FT-IR spectroscopy based on ASTM E168 standard, which involves mixing five milligrams of analyst with about 100 mg of dried potassium bromide and an appropriate amount of the pellet was prepared by compression. The pellet was placed in the incident IR beam path of varying frequency, subsequently, resonant absorbed by the molecules resulted in a percentage transmission being detected in the FT-IR detector. Finally, the FT-IR spectrum was obtained over the region 400-4000 cm^{-1}.

2.3.4. Scanning Electron Microscopy (SEM) Characterization

The synthesized HAp morphology, particle size distribution and microstructure were studied using SEM based on ASTM E986-97 standard. This involved coating the sample with platinum and subsequently attaching it on a pure copper sample holder, which was put in the SEM that operated under vacuum at the pressure of 2.5 MPa and an image pattern in the topography form was generated.

3. Results

The XRD spectra obtained from the dolomite (D) and dolomite-based HAp (DHAp) were presented in Figure 1 while XRF results were summarized in Table 1. The crystal size (D_{hkl}), surface area and crystallinity for DHAp were calculated from X-ray diffractogram data and were presented in Table 2. In addition, their unitary cell parameter (a, c) and unit cell volume (V) were presented in Table 3 while the Ca/P ratio of the DHAp was summarized in Table 4. Furthermore, FT-IR spectrum of DHAp was shown in Figure 2 while the wave number and chemical group of FT-IR absorbtion bands were briefed in the Table 5. Also, representative SEM micrograph of the obtained HAp was presented in Plate 1.

4. Discussion

The elemental and structural analyses of the dolomite as-received in this study were discussed using XRF and XRD results. Also, chemical properties analysis and morphologyof the synthesized dolomite-based HAp were discussed using results from XRF, XRD and SEM.

4.1. Analysis of the Physicochemical Properties of Dolomite and Dolomite-Based HAp

- **The dolomite and dolomite-based hydroxyapatite XRD Spectra**

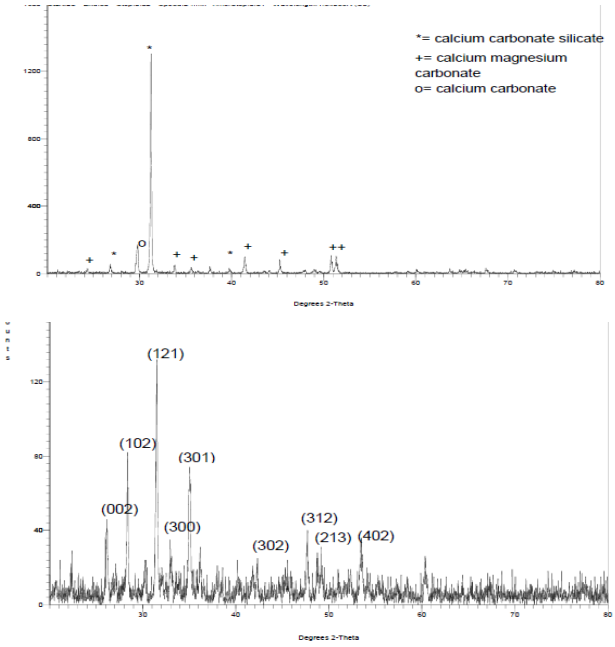

Figure 1. XRD spectrum of (a) dolomite (b) dolomite-based Hap

Table 1

Component (Symbol)	D Wt%	DHAp Wt.%
O		37.7
Mg	1.8	1.2.
Al	0.2	1.4
Si	0.4	0.9
P	0.2	13.1
Cl		0.5
S	0.3	0.0
Ca	41.6	45.7
Fe	0.6	0.1
Mo	0.1	
Zn	0.1	0.1
Sn	2.8	0.2
Sb	2.4	

Table 2. Experimental Diffraction Angles, Crystal Size, Surface Area, % Crystallinity of Dolomite-based Hydroxyapatite

$2\Theta_B$	$B=\Theta_2-\Theta_1$	hkl	Crystal size (nm)	Surface Area (m^2/g)	Crystallinity (%)
26.14	0.06	002	137.9	13.769	80
28.34	0.04	102	204.7	9.2765	80
31.5	0.06	121	155.2	12.23	80

Table 3. Unitary Cell Parameters of Synthesized Dolomite-based Hydroxyapatite

Sample	a= b (Å)	c (Å)	c/a	U	V
DHAp	9.4088	6.814	0.7241	0.361	521.74

Table 4. The Ca/P Ratio of the Synthesized Dolomite-based Hydroxyapatite

Hydroxyapatite	Symbol	Ca/P
Dolomite-based HAp	DHAp	2.70

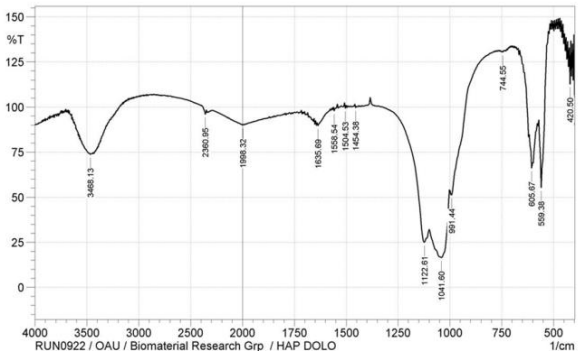

Figure 2. The FT-IR spectrum of dolomite-based hydroxyapatite

Table 5. The Wave Number and Chemical group of FT-IR Absorbtion Band for the Dolomite-based hydroxyapatite

S/N	Associated FT-IR wave number (cm^{-1})	Molecules
1	420.5, 599.4, 603.6	v_4 (P-O)
2	1122.6, 1041.6, 991.4	V_3 (P-O)
3	2361.0, 2165.6,	C-O (gaseous CO_2)
4	1998.32	Symmetric stretching of HPO_4^{-2}
5	3468.1	OH^- bond

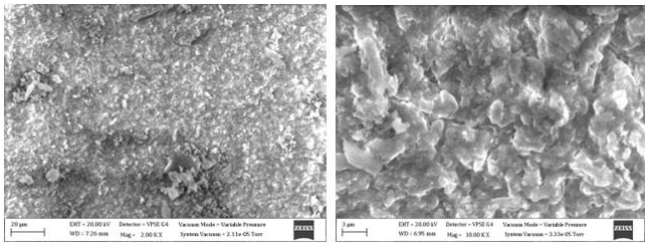

Plate 1. SEM micrograph of dolomite-based hydroxyapatite of Magnification (a) 2000x and (b) 10000x

The XRD and XRF spectroscopy were used to analyze the dolomite as received and dolomite-based HAp as shown in Figure 1 and Table 1 respectively. The XRD patterns were similar to XRD pattern of calcite ($CaCO_3$) with the peaks 29.60 ° (104), which matched with the primary reference JCPD card no. 00-002-0629. Also, peaks of calcium carbonate silicate was also observed with the following peaks 26.76 °(130), 31.23 °(-511) and 39.84 °(-531), which were similar to JCPD card no. 00-13-0416. Also, the calcium magnesium carbonate was observed with the following peaks 24.220 (012), 33.76 ° (006), 35.6 °(015), 37.6 °(110) 41.42 °(113), 45.2 °(202), 50.8 °(018) and 51.4 °(116), which matched with standard reference JCPD card no. 00-036-0426 of calcium magnesium carbonate. This result was corroborated with XRF results in which dolomite had calcium contents of 41.61 %, silicon content of 0.4234 % and magnesium (Mg) content of 1.81 wt. %.

The result obtained from the XRD characterization of DHAp was shown in Figure 1. According to the XRD spectrum of the HAp synthesized, the spectrum showing the diffraction maxima corresponding to HAp phase (JCPDS) at peaks 26.1 °(002), 31.5 °(121) and 33.0 ° (300) in 2Θ for dolomite-based HAp. The hexagonal crystal structure was identified based on the XRD results, which was in agreement with the JCPD Card No. 01-075-3728. This result was also confirmed by the calculated unitary parameters, c= 6.814 Å and a= 9.4088 Å, in Table 3, which showed insignificant diversion from the stoichiometric hydroxyapatite (c = 6.8745 Å and a= 9.4166 Å) [32]. Furthermore, the HAp had narrow peaks, which signifies big particle size and high crystallinity. This observation was also revealed in the calculated crystal size and % crystallinity summarized in Table 2. It can be seen that the particle size was not even, which is one of the feature of wet chemical precipitation product. This result was supported by FT-IR and XRF results.

- **The elemental analysis of the hydroxyapatite synthesized from dolomite using XRF techniques**

The XRF result analysis of the obtained dolomite-based HAp was summarized in Table 1, which showed the purity of the synthesized HAp. Qualitatively, the sample contained primary Ca, P and O compounds as expected from hydroxyapatite. Also, beneficial elements, such as Mg^{2+}, Al^{3+}, Si^{2+} and Zn^{2+}, exist in trace amount, which has been shown to accelerate the process of bone formation [35]. Researches have found that presence of silicon in synthetic HAp increases cell growth density while strontium ion improved osteoblast activity and differentiation, and also subdued osteoclast proliferation and creation [20]. This indicates that the synthesized materials will function well as bone substitite.

Furthermore, the quantitative analysis of HAp in terms of calcium phosphorous (Ca/P) molar ratio was calculated as shown in Table 4. From the Table, it can be observed that HAp Ca/P ratio was 2.70, which was above the theoritical value of 1.67. This observation was attributed to the presence of trace element in HAp, which is one of the features of natural HAp. Studies have shown that the substitution by trace element occurs at the phosphate ion site by anions, such as CO_3^{2-} and SO_3^{2-} while calcium ion site can be replaced by cations, such as Mg^{2+}. Previous investigation on the Ca/P ratio of HAp extracted from human bone was above 2.0, which is attributed to the presence of trace element in the natural hydroxyapatite [36]. Hence, the dolomite-based HAp will function well as bone substitute. In addition, evaluation of element with atomic number (Z) less than 11 is, however, impossible with this technique. Hence, element, such hydrogen, was not visible. However, the presence of these elements can be shown in the FT-IR spectrum.

- **The synthesized dolomite-based hydroxyapatite FT-IR spectrum**

The FT-IR spectrum of the dolomite-based hydroxyapatite (DHAp) revealed in Figure 2 and its characteristic bands was summarized in Table 5. From the observation gotten from the figure, the FT-IR spectrum revealed the triply degenerate v_3 domain detected at peaks 1123, 1042 and 991 cm^{-1}, which represents main signal of phosphate (P-O) stretching asymmetric adsorption coming from PO_4^{3-}. These peaks were similar to the one observed by [6,23]. The anti-harmonic bending motion absorption bands of v_4 phosphate compound were also observed at 606 cm^{-1} in DHAp [6]. The presence of hydroxyl bond was shown by the peak at 3468.1 cm^{-1}. The absence hydroxyle lattice bond at peak 3570.1cm^{-1} was attributed to the Mg ion substitution in the Ca ion lattice site of HAp [8]. According to [8] and [37] substitution of Ca^{2+} and PO_4^{3-} by species, such as Mg^{2+} and CO_3^{2-}, respectively is known to induce vacancy in OH^- site leading to low concentration of OH^- in the HAp lattice structure, and hence diminished OH^- diagnostic peak of FT-IR. Also, hydroxyl (OH^-) ions may be replaced by carbonate ions, which will cause decrease in the major peaks intensity and eventually total disappearance of OH^- stretching and librational bands at 3570 and 631 cm^{-1} respectively. This implies that DHAp synthesized contains trace element that substituted either Ca ion or phosphate ion, which brings about the reduction of hydroxyl ion in the lattce. However, this effect might improve bone regeneration since substitution increases the roughness of the hydroxyapatite stucture thereby increasing large surface area for osteoconduction and proliferation in bone regeneration. Hence, the synthesized DHAp will function well in bone regeneration.

- **Morphology of dolomite-based hydroxyapatite**

The sample surface morphology was studied through the corresponding SEM micrograph, which employ an accelerating voltage of 20 kV and a magnification of 2000x, as shown in Plate 1. Based on the morphology, dolomite-based HAp had rod-shape structures of varying sizes that resulted to rough surface, which was similar to natural bone microstructure.

5. Conclusions

The study concluded that hydroxyapatite was successfully synthesized from Nigerian-based dolomite based on the results of elemental, chemical and morphological characterizations. The results, furthermore, support the hypothesis that the HAp synthesized from dolomite may be suitable for bone regeneration.

ACKNOWLEDGEMENTS

The authors gratefully acknowledge the financial support from Tertiary Education Trust Fund (TETFUND).

REFERENCES

[1] Osuchukwu, O. A.; Salihi, A.; Abdullahi, I; Abdulkareem, B. and Nwannenna, C. S. Synthesis Techniques, Characterization and Mechanical Properties of Natural Derived Hydroxyapatite Scaffolds for bone Implants: A Review, *SN Applied Science* 2021, vol. 3, pp. 822.

[2] Agrawal, K., Singh, G., Puri, D. and Prakash, S. Synthesis and Characterization of Hydroxyapatite Powder by Sol-gel Method for Biomedical Application. *Journal of Materials Characterisation and Engineering*, 2011, vol. 10, no. 8, pp. 727-734.

[3] Rujitanapanich, S.; Kumpapan, P. and Wanjanoi, P. Synthesis of Hydroxyapatite from Oyster Shell via Precipitation. *Energy Procedia* 2014, vol. 56, pp. 112-117.

[4] Ma, G. Three Common Preparation Methods of Hydroxyapatite. *IOP Conf. Series: Materials Science and Engineering 2019*, vol. 688, pp. 033057.

[5] Azis, Y.; Adrian, M.; Alfarisi, C. D.; Khairat and Sri, R. S. Synthesis of Hydroxyapatite Nanoparticles from Egg Shell by Sol-Gel Method, IOP Conf. Series: *Materials Science and Engineering* 2018, vol. 345, pp. 012040.

[6] Sirait, M.; Sinulingga, K.; Siregar, N. and Siregar, R. S. Synthesis of Hydroxyapatite from Limestone, by Precipitation Method. *Journal of Physics* 2020, vol. 1462, pp. 1-9.

[7] Algamal, Y.; A.; Khalil; Amna S. and Mohammed, B. A. Antimicrobial Activity of Hydroxyapatite Nanoparticles Prepared From Marble Wastes. *Main Group Chemistry*, 2022, vol. 21, pp. 865-873.

[8] Mahene, W. L.; Gervas, C.; Hilonga, A. H.; and Machunda, R. L. Synthesis and FT-IR Characterization of Mg-Hydroxyapatite derived from Dolostone with High Dolomite Mineral Content. *Tanzania Journal of Science*, 2020, vol. 46, pp. 661-672.

[9] Fatoye, F. and Gideon, Y. Geology and Occurrences of Limestone and Marble in Nigeria. *Journal of Natural Science Research* 2013, vol. 3, pp. 60-61. doi:10.10881757-899X345/ 1012040.

[10] Omoseebi, A. O. and Tanko, I. Y. Geochemistry and Determination of Mineral Properties of Dolomite Deposit in Ikpeshi Southern. Nigeria. *European Journal of Environment and Earth Sciences* 2021, vol. 2, pp. 41-46. DOI: http://dx.doi.org/10.24018/ejgeo.2021.2.5.175.

[11] Akande, J. M. and Agbalajobi, S. A. Analysis on Some Physical and Chemical Properties of Oreke Dolomite Deposit. *Journal of Minerals and Materials Characterization and Engineering*, 2013, vol. 1, pp. 33-38.

[12] Johnson, A. D.; Cosmas, A.; Adekunle, E.; Akinmutade, J. O, and Obabiyi, Y. Determination of the Mineralogical Composition of Dolomite Deposit of Ikpeshi, Akoko Edo L. G. A., Edo State, for Industrial Applications, *IOSR Journal of Mechanical and Civil Engineering* 2025, vol. 22, pp. 08 - 18.

[13] Pu'ad, M. N. A. S.; Haq, A. R. H.; Noh, M.; Abdullah, H. Z.; idris, M. I. and Lee, T. C. Synthesis Method of Hydroxyapatite: A Review, Material Today: Proceedings, 2020 https://doi.org/10.116/j.matpr.2020.05.536.

[14] Jamarun, N.; Azhaman, Z.; Zilfa and Septiani, O. Effect of Firing for the Synthesis of Hydroxyapatite from Precipitation Method. *Oriental Journal of Chemistry* 2016, vol. 32, pp.

2095-2099.

[15] Nayak, A. K. Hydroxyapatite Synthesis Methodologies: An Overview, *Chem Tech 2010*, vol. 2, 903-907.

[16] Rial, R.; Gonzale-Durruthy, M.; Liu, Z. and Ruso, J. M. Review: Advanced Materials Based on Nano-sized Hydroxyapatite. *Molecule* 2020, vol. 26, pp. 1-22.

[17] Ma, G. Three Common Preparation Methods of Hydroxyapatite preparation. *IOP conf. Ser. Mater. Sci. Eng* 2019, vol. 688, no. 033057, pp. 1-13.

[18] Cox, S. Synthesis Method of Hydroxyapatite, *ceram* 2014.

[19] Massit, A.; Yacoubi, A. E.; Kholtei, A.; Idrissi, B. C. XRD and FTIR Analysis of Magnesium Substitute Tri-calcium Calcium Phosphate Using a Wet Precipitation Method. *Biointerface Research in Applied Chemistry* 2021, vol. 11, pp. 8034-8042.

[20] Pu'ad, N. M.; Koshy, P. and Abdullah, H. Synthesis of Hydroxyapatite from Natural Source, *Heligon* 2019, vol. 5, pp. 1-15.

[21] Indrani, D.; Soegdono, B.; Adi, W. and Tout, N. Phase Composition and Crystallinity of the Hydroxyapatite. *International Journal of Pharmacy* 2017, vol. 9, pp. 87-91.

[22] Milev, A. S.; Kannangara, G. S. K. and Wilson, M. A. Template-Directed Synthesis of Hydroxyapatitee from a Lamellar Phosphonate Precursor. *Langmuir* 2003 vol. 20, pp. 1888-1894.

[23] Habibah, T. U.; Amlani, D. V.; Brizuela, M. Hydroxyapatite Dental Material, *International Journal of Biomedical Materials Research* 2019, vol. 12, pp. 1-6 https://doi.org/10.116.

[24] Rial, R.; Gonzale-Durruthy, M.; Liu, Z. and Ruso, J. M.; "Review: Advanced Materials Based on Nanosized Hydroxyapatite," *Molecule* 2020, vol. 26, pp. 1-22.

[25] Rodriguez-lugo, V.; Karthik, T. V. K.; Mendoza-Anaya, D.; Rubio-Rosas, E.; Ceron, L. S. V.; Reyes-Valderrama, M. I. and Salinas-Rodriguez, E. Wet Chemical Synthesis of Nano-crystalline Hydroxyapatite Flakes: Effect of pH and Sintering Temperature on Structural and Morphological Properties, *Royal Society of Chemistry* 2018,vol. 5, pp. 1-14.

[26] Wang, P.; Li, C.; Gong, H.; Jiang, H. and Li, K. Effect of Synthesis Condition on the Morphology of Hydroxyapatite Nanoparticles Produced by Wet Chemical Process. *Powder Technology* 2010, vol. 203, pp. 315-321. doi: 10.1016/j.powtec.2010.05.023.

[27] Rafie, S. M. and Nordin, D. Synthesis and Characteristic of Hydroxyapatite Nanoparticles. *Malaysia Journal of Analytical Science* 2017, vol. 21, pp.136-148.

[28] Jamarun, N.; Arhaman, Z.; Arief, S. and Sari, T. Effect of Temperature on the Synthesis of Hydroxyapatite from Limestone, *Rasayan J. Chem* 2015, vol. 8, pp. 133-137.

[29] Alias, M.; Hamzah, S. and Saidin, J. The effect of Sintering Temperature on the Characteristic and Properties of Hydroxyapatite Extracted from Fish Scale Bio-waste. *International Journal of Engineering and Technology* 2018, vol. 7, pp. 1-5.

[30] Gyorgy, S.; Karoly Z.; Fazekas, P.; Nemeth, P.; Bodies, E.; Menhard, A.; Kotai, L. and Klebert, S. Effect of the Reaction Temperature on the Morphology of Nanosized Hydroxyapatite, *Journal of Thermal Analysis and Calorimetry* 2019, vol. 138 pp. 145-151.

[31] Kazemzadeh, R.; Behnamghader, A. and Hesaraki, S.; "Effect of Synthesis Temperature on the Phase and Morphological Characteristics of Hydroxyapatite Nanoparticles," *Advanced Material Research* 2011, vol. 264-265, pp. 1329-1333.

[32] Trigo, J. B.; Jimenez-Flores, Y.; Suarez, V.; Suarez, V.; Suarez-Quezada, M. and Nogal, U. Powder Technology: Sol-gel Synthesis of Calcium Deficient Hydroxyapatite Influence of pH Behavior during the synthesis of Structural and Chemical Composition and Physical Properties. Cavalheiro A. A.: London, United Kingdom, 2018. doi: 10.5772/intechopen.76531.

[33] Scalera, F.; Geraso, F.; Sanosh, K. P.; Sannino, A. and Licciulli, A.; Z. Influence of the Calcination Temperature on the Morphological and Mechanical Properties of Highly Porous Hydroxyapatite Scaffold. *Ceramic International* 2013, vol. 39, pp. 4839-4846.

[34] Senthilarasan, K. and Sakthivel, P.; Synthesis and Characterization of Hydroxyapatite with Gum Arabic (Biopolymer) Nano Composites for Bone Repair, *International Journal of Science and research* 2012, vol. 3, pp. 2643-2647, 2012. ISSN (Online): 2319-7064.

[35] Hussin, M. S. F.; Abdullah, H. Z.; Idris M. I. and Wahap M. A. A. Extraction of Natural Hydroxyapatite for Biomedical Applications-A Review. *Heliyon* 2022 vol. 8, e10356.

[36] Londolo-Restrepo, S. M.; Jeronimo-Cruz, R.; Millan-Malo, B. M.; Rivera-Munoz, E. M. and Rodriguez-Garcia, M. E. Effect of the Nano-crystal Size on the X-ray Diffraction Patterns of Biogenic Hydroxyapatite from Human, Bovine and Porcine Bones. *Scientific Report* 2019, vol. 9. pp. 1-12.

[37] Murugesa, M.; Nagamony, P. and Viswanathan, C. Core-shell hydroxyapatite/Mg nanostructures: Surfactant free facile synthesis, characterization and their in-vitro cell viability studies against leukaemia cancer cells (K562). *RSC Advances* 2015, vol. 5, pp. 48705-48711.